Free Radical Research, November 2006; 40(11): 1138–1148

informa
healthcare

UV-irradiation induces oxidative damage to mitochondrial DNA primarily through hydrogen peroxide: Analysis of 8-oxodGuo by HPLC

DAISAKU TAKAI[1], SANG-HEE PARK[1], YASUNARI TAKADA[1], SHIZUKO ICHINOSE[2], MASANOBU KITAGAWA[3], & MAKOTO AKASHI[1]

[1]*Department of Radiation Emergency Medicine, National Institute of Radiological Sciences, Chiba, Japan,* [2]*Instrumental Analysis Research Center, Tokyo Medical and Dental University, Bunkyo-ku, Tokyo, Japan, and* [3]*Department of Comprehensive Pathology, Graduate School, Tokyo Medical and Dental University, Bunkyo-ku, Tokyo, Japan*

Accepted by Professor B. Halliwell

(Received 7 January 2006; in revised form 4 June 2006)

Abstract

Roles of reactive oxygen species (ROS) in damage to mitochondrial DNA (mtDNA) following ultraviolet (UV)-irradiation were investigated in the human hepatoma cell line SK-HEP-1. We altered the intracellular status of ROS by the overexpression of manganese superoxide dismutase (MnSOD) and/or catalase. Using HPLC, we analyzed 8-oxo-7,8-dihydro-2′-deoxyguanosine (8-oxodGuo), known as a marker of damage to DNA molecules. UV-irradiation resulted in the accumulation of 8-oxodGuo in these cells. The overexpression of MnSOD enhanced the accumulation of 8-oxodGuo by UV. The co-overexpression of catalase inhibited the accumulation of 8-oxodGuo by UV in MnSOD-transfectants. The overexpression of MnSOD reduced the colony forming capacity in SK-HEP-1 cells and the co-overexpression of catalase with MnSOD stimulated the capacity compared to control. UV-irradiation inhibited the colony forming capacity in these cells; no difference was observed among the capacities of control, MnSOD- and catalase-transfectants. However, the overexpression of MnSOD/catalase significantly rescued the reduction of colony forming capacity by UV-irradiation. Our results suggest that the accumulation of hydrogen peroxide plays a key role in the oxidative damage to mtDNA of UV-irradiated cells, and also that the overexpression of both MnSOD and catalase reduces the mtDNA damage and blocks the growth inhibition by UV. Our results also indicate that the increased activity of MnSOD may lead to a toxic effect on mtDNA by UV-irradiation.

Keywords: *Hydrogen peroxide, mitochondrial DNA (mtDNA), 8-oxo-7,8-dihydro-2′-deoxyguanosine (8-oxodGuo), reactive oxygen species (ROS), UV-irradiation*

Introduction

Reactive oxygen species (ROS) are physiologically generated as a consequence of aerobic respiration and substrate oxidation in aerobic organisms; the generation is increased in response to external stimuli. Excessive accumulation of ROS results in oxidative stress that leads to damage to biological macromolecules. ROS can cause DNA damage, resulting in genetic mutations [1]. The mitochondrial respiratory chain is a powerful source of ROS, and ROS are considered to be the pathogenic agents of many diseases and of aging. Mammalian mitochondria account for over 90% of cellular oxygen consumption, and 1–5% of consumed oxygen in mitochondria is converted to ROS in the mitochondrial respiratory chain [2,3]. The implication of mitochondria both as producers and targets of ROS is thought to be the basis for the mechanisms of aging [3,4], suggesting

Correspondence: M. Akashi, Department of Radiation Emergency Medicine, National Institute of Radiological Sciences, 4-9-1 Anagawa, Inage-ku, Chiba-city, Chiba 263-8555, Japan. Tel: 81 43 206 3122. Fax: 81 43 284 1736. E-mail: akashi@nirs.go.jp

ISSN 1071-5762 print/ISSN 1029-2470 online © 2006 Informa UK Ltd.
DOI: 10.1080/10715760600838381

that random alterations of mitochondrial DNA (mtDNA) in somatic cells are responsible for the energetic decline accompanying senescence. However, eukaryotic cells have inherent defensive mechanisms to counterbalance the adverse effects exerted by ROS; they contain enzymatic systems capable of converting ROS into less toxic or nontoxic species. Manganese superoxide dismutase (MnSOD, EC 1.15.1.1) is an enzyme located in mitochondria, and it is responsible for converting superoxide anions to hydrogen peroxide (H_2O_2). Glutathione peroxidase (GSH-Px, EC 1.11.1.19), catalase (EC 1.11.1.6) and peroxiredoxin (EC1.11.1.7) convert H_2O_2 to harmless water. Transfection of MnSOD cDNA has been reported to render cells resistant to tumor necrosis factor α- irradiation-, or adriamycin-mediated cytotoxity and irradiation-induced neoplastic transformation [5], whereas increased activities of MnSOD lead to the accumulation of H_2O_2 if it cannot be converted, in turn, by the increased activity of catalase or GSH-Px. Moreover, it has been shown that MnSOD-transgenic mice were resistant against oxygen-induced injury and toxicity as compared to control mice [6]. Thus, the precise mechanism for damage by ROS still remain largely unknown.

Eukaryotic cells contain mitochondria that generate most of the energy necessary for life. Mitochondria have their own genome, mtDNA, approximately 16-kbp DNA in human cells, that encodes subunits of the mitochondrial electron transport system and the rRNAs and tRNAs used for constructing the mitochondrial translational machinery. MtDNA is a closed circular double-stranded DNA that is replicated within mitochondria by DNA polymerase gamma [7]. Each subunit encoded by mtDNA is essential for normal oxidative phosphorylation and hence for a large part of ATP production in a cell. Many studies have shown that mutations in mtDNA occur in a wide variety of degenerative diseases, not only particular genetic diseases but also neurodegenerative disorders, diabetes, cancer and aging [8,9]. While the mechanisms for mutations in mtDNA are still unclear, it is suggested that many of them result from oxidative damage via ROS [10]. Since mtDNA is located in the matrix near the inner mitochondrial membrane and is constantly exposed to ROS produced by aerobic respiration, mtDNA is thought to be several times more vulnerable to oxidative damage and the subsequent mutations more easily generated compared with nuclear DNA [11]. Unlike nuclear DNA, on the other hand, mtDNA lacks histones and other DNA-associated proteins and is continuously replicated, even in terminally differentiated cells such as nerve cells and cardiomyocytes. Furthermore, because mtDNA lacks introns, the probability of oxidative modification of a coding region is very high. Therefore, somatic mtDNA damage potentially causes more adverse effects on cellular functions than does somatic nuclear DNA damage. It stands to reason, then, that detection of mtDNA damage, especially that caused by ROS, is extremely important.

Previous studies have found that 8-oxo-7,8-dihydro-2′-deoxyguanosine (8-oxodGuo), an oxidatively modified guanine base, accumulates and increases rapidly in mtDNA [12], suggesting that it is a good indicator of oxidative damage in mtDNA. Ultraviolet (UV) rays are known to induce the generation of ROS [13,14] and to cause point mutations and large-scale deletion mutations in mtDNA [15,16]. In the present study, human MnSOD and/or catalase cDNAs were introduced into a human hepatoma cell line, SK-HEP-1, in order to modulate the cellular redox status. We then studied the mechanisms for mtDNA damage by ROS using high performance liquid chromatography (HPLC) for the quantitative analysis of 8-oxodGuo. We showed for the first time that mtDNA damage occurs mainly via H_2O_2 in UV-irradiation. We also showed that the overexpression of MnSOD and catalase effectively rescues the mtDNA damage and growth inhibition induced by UV-irradiation.

Materials and methods

Reagents

Nitro blue tetrazolium (NBT) and diethylenetriamine pentaacetic acid were obtained from Nacalai Tesque (Kyoto, Japan). Riboflavin, peroxidase, hydrogen peroxide (H_2O_2), 3,3′-diaminobenzidine (DAB), DNase I, nuclease P1, bacterium alkaline phosphatase, agarose and sodium acetate were obtained from Wako Pure Chemical Industries (Osaka, Japan). Giemsa solution was obtained from MERCK (Darmstadt, Germany). 5-(and-6)-chloromethyl-2′,7′- dichlorodihydrofluorescein diacetate, acetyl ester (CM-H_2DCFDA) and calcein-acetoxymethyl ester (AM) were obtained from Molecular Probes (Eugene, OR). TaKaRa Ex Taq™ was obtained from TaKaRa Bio Inc. (Otsu, Japan).

Cells and cell culture

Human hepatoma cells, SK-HEP-1, were cultured in alpha-MEM (COSMO BIO, Tokyo, Japan) supplemented with 7% fetal calf serum (Intergen, Purchase, NY), 50 units/ml penicillin G sodium and 50 μg/ml streptomycin sulfate (Gibco, Invitrogen Corp., CA) in a humidified atmosphere containing 5% CO_2.

Construction of expression vectors and transfection

An expression vector of human MnSOD was constructed as described previously [17]. For a

catalase expression vector, human catalase cDNA (1.6 kbp Hind III fragment of pCAT10 containing the coding region, originally from American Type Tissue Culture Collection, Manassas, VA) was cloned into either pcDNA3.1/Neo or pcDNA3.1/Zeo vector (Invitrogen, Carlsbad, CA). For each experiment, one microgram of plasmid was introduced into 10^5 cells using FuGENE6 (Roche Diagnostics, Mannheim, Germany). Twenty-four hours after exposure to DNA, cells were cultured in selection media supplemented with either 0.8 mg/ml of G418 (Boehringer Manheim Biochemicals, Indianapolis, IN) or 0.4 mg/ml Zeocin (Invitrogen Corp, Carlsbad, CA) for 3 weeks. Single colonies of G418- or Zeocin-resistant cells were isolated and then screened for the levels of MnSOD or catalase activity by native gel assay.

Native gel assay

Cells were sonicated in ice-cold potassium phosphate buffer (50 mM, pH 7.0) with diethylenetriamine pentaacetic acid and protease inhibitor cocktail (COMPLETE™-EDTA free, Roche Diagnostics, Mannheim, Germany). After centrifugation at 14,000*g* for 15 min, protein concentrations in the supernatants were determined using Bio-Rad Protein Assay (Bio-Rad, Hercules, CA) with bovine serum albumin as the standard. For SOD activity assay, proteins of each sample (40 μg) were separated by 12% non-denatured polyacrylamide gel electrophoresis. The gel was stained by incubation with 2.4 mM NBT for 15 min in the dark, followed by soaking in 36 mM riboflavin under fluorescent light to photogenerate ROS. Chromatic bands corresponding to SODs appeared against a blue background (reduced products of NBT). For catalase activity, proteins of each sample (40 μg) were separated by 7.5% non-denatured polyacrylamide gel electrophoresis. The gel was rinsed in 50 μg/ml of peroxidase for 45 min followed by adding 5 mM H_2O_2 and rinsed for 15 min. Then the gels were stained in 0.5 mg/ml DAB. Chromatic bands corresponding to catalase appeared against a brown background. The relative densities of all bands were determined by Intelligent Quantifier™ (BioImage Systems, Ann Arbor, MI).

Transmission electron microscopy

Cells were fixed with 2.5% glutaraldehyde in 0.1 M PBS at 4°C overnight and post-fixed with 1% OsO_4 buffered with 0.1 M PBS for 2 h. The cells were dehydrated in a graded series of ethanol and embedded in Epon 812. Ultrathin (90 nm) sections were collected on copper grids, double stained with uranyl acetate and lead citrate, and then examined by transmission electron microscopy (H-7100, Hitachi, Hitachinaka, Japan).

Immunoelectron microscopy

Cells were fixed in 4% paraformaldehyde in 0.1 M phosphate buffer (pH 7.4) for 15 min. The cells were dehydrated and embedded in LR White resin (London Resin, Reading UK). Ultrathin sections were prepared and mounted on nickel grids. After incubation with 10% normal goat serum for 10 min, the sections were incubated overnight at 4°C with the anti-catalase antibody (Calbiochem, EMD Biosciences, Darmstadt, Germany). After being washed with PBS, the sections were incubated with a mixture of a goat anti-rabbit IgG conjugated to 10-nm-diameter gold particles (1:50, British Biocell International, Cardiff, UK) for 2 h at 4°C. The sections were then washed with water and stained with uranyl acetate. The sections were examined with electron microscope, H-7100.

Isolation of mitochondria and purification of mitochondrial DNA

Mitochondria from SK-HEP-1 cells were isolated by sucrose gradient centrifugation as described previously, with slight modifications [18]. Cells were plated in a 100-mm culture dish for 24 h. The culture medium was then removed and the cells were irradiated with UV (254 nm) at 1 kJ/m^2 in an irradiation chamber (FUNA®-UV Crosslinker FS-800, Funakoshi, Tokyo, Japan). Immediately after irradiation, 1×10^8 cells were washed with PBS and homogenized in ice-cold medium containing 150 mM $MgCl_2$, 10 mM KCl and 10 mM Tris–HCl (pH 6.7) with a homogenizer. After adding sucrose (final concentration to 0.25 M), the homogenate was centrifuged at 1000*g* for 1 min. The supernatant was further centrifuged at 10,000*g* for 10 min. The resulting mitochondrial pellet was re-suspended in ice-cold homogenization medium and incubated with DNaseI to digest nuclear DNA contaminated in the pellet for 15 min at 37°C [19].

MtDNA was purified from isolated mitochondria using silica-gel-membrane without organic extraction (DNeasy® kit, QIAGEN, Hilden, Germany). The mitochondrial pellet was suspended in lysis buffer containing proteinase K and incubated at 70°C for 10 min. After adding 200 μl of ethanol, the sample was loaded onto the DNeasy spin column and centrifuged at 6000*g* for 1 min. After discarding a flow-through, the DNeasy membrane was washed with washing buffer. Then elution buffer was loaded onto the DNeasy membrane and incubated at room temperature for 1 min. Finally, the column was centrifuged at 6000*g* for 1 min to elute DNA.

In order to check the contamination of nuclear DNA in the purified mtDNA, the 196 bp region of a nuclear DNA encoded glyceraldehydes-3-phosphate dehydrogenase (G3PDH) gene was amplified using

PCR. The sequences of the PCR primers were as follows: forward, 5′-CCAT GGAG AAGG CTGG GGCT C-3′; reverse, 5′-CCAA AGTT GTCA TGGA TGAC C-3′. DNA amplifications were carried out by TaKaRa Ex Taq™ in a thermal cycler (Master Cycler Gradient, Eppendorf, Hamburg, Germany) with a denaturing step at 94°C for 1 min, the step cycle set for 30 cycles (with each cycle consisting of denaturing 94°C for 30 s, annealing at 60°C for 30 s, and extension at 72°C for 1 min), followed by a final extension step at 72°C for 10 min. The PCR products were tested by 2% agarose gel electrophoresis and staining with ethidium bromide.

Cell growth analysis

The cell growth rate was determined by a colorimetric assay based on the cleavage of tetrazolium salt WST-1 (4-[3-(4-Iodophenyl)-2-(4-nitrophenyl)-2H-5-tetrazolio]-1, 3-benzene disulfonate) by mitochondrial dehydrogenases in viable cells (Roche Diagnostics). Cells were seeded at an initial concentration of 200 cells/well in a 96-well microplate and cultured in medium. Then WST-1 was added to the cultures and incubated at 37°C for 4 h. The production of formazan was measured by microplate reader (Wallac 1420 ARVO™sx, PerkinElmer Life Science, Boston, MA) at a wavelength of 480 nm.

Colony formation assay

Two hundreds to a thousand cells were plated in a 60-mm culture dish for 24 h. The culture medium was then removed and cells were irradiated with UV (254 nm) at 0–40 J/m^2 in an irradiation chamber and cultured in medium for 7 days. Then the cells were fixed in methanol and stained with Giemsa solution. Stained colonies were counted using the software Intelligent Quantifier™ (BioImage Systems).

Analysis of ROS production

Intracellular ROS production was assessed by oxidation of CM-H_2DCFDA and measurement by flowcytometer [20]. Cells were incubated with 2 μM CM-H_2DCFDA in PBS for 15 min at 37°C and harvested. Resuspended cells were subjected to flowcytometric analysis (FACSCalibur™, Becton Dickinson, Franklin Lakes, NJ). The excitation wavelength was 488 nm, and the observation wavelength was 530 nm for green fluorescence.

Measurement of oxidative damage of DNA by HPLC-ECD

MtDNA was heat-denatured and digested by nuclease P1 in 20 mM sodium acetate (pH 4.5) for 1 h at 37°C. The digested samples were then treated with bacterial alkaline phosphatase for 1 h at 37°C and analyzed for 8-oxodGuo by HPLC-8020 system (TOSOH, Tokyo, Japan) with a reverse-phase chromatography column, TSK gel ODS-80Ts QA column (TOSOH). The elution buffer was 10% methanol in 50 mM sodium acetate (pH 5.2) and the flow rate was 1 ml/min. 8-oxodGuo was detected by electrochemical detector EC-8020 (TOSOH), and 2′-deoxyguanosine (2dG) was simultaneously monitored at 260 nm by UV detector UV-8020 (TOSOH). As standard, 8-oxodGuo commercially available was used (Wako Pure Chemical Industries, Ltd. Osaka, Japan). The detected peaks were analyzed by MultiStation LC-8020 Model II (TOSOH).

Measurement of intracellular chelatable iron release

The intracellular levels of chelatable iron were measured using calcein, a fluorescent metal-sensitive probe. Cells were UVC-irradiated at a dose of 1 kJ/cm^2 and incubated with 0.05 μM calcein-AM in DMEM medium for 15 min at 37°C. Then the cells were washed with PBS containing 10% FCS and resuspended in 10 mM Hepes buffer containing 2 mM diethyltriaminepentaacetic acid. The calcein fluorescence of cells was measured by a spectro-fluorometer with excitation at 488 nm and emission at 517 nm.

Western blot analysis

Cells were lysed in buffer containing 50 mM Tris–HCl (pH 8.0), 150 mM NaCl, 3 mM NaN_3, 0.1% (w/v) SDS, 1% (v/v) Nonidet P-40 and 0.5% sodium deoxycholate. The protein concentration of each sample was measured and electrophoresis was performed with samples containing 120 μg of cell lysates in SDS-PAGE loading buffer using 12% polyacrilamide gel, followed by transfer of the proteins onto pure nitrocellulose membranes (Trans-Blot Transfer Membrane, Bio-Rad). Immunoreactivity was detected by enhanced chemiluminescence (Amersham Biosciences).

Results

Activities of MnSOD and catalase in SK-HEP-1 cells overexpressing MnSOD and/or catalase

To study the role of ROS in UV-irradiated cells, we first transfected a pCR3.1/Neo construct containing either a full-length cDNA of human MnSOD or catalase to the human hepatoma cell line, SK-HEP-1 [17]. As a control, cells were transfected with pCR3.1/Neo vector. After selection, we obtained several clones resistant to G418 of each transfectant. Next, the control cells and MnSOD-transfectants were transfected with a pCDNA3.1/Zeo construct

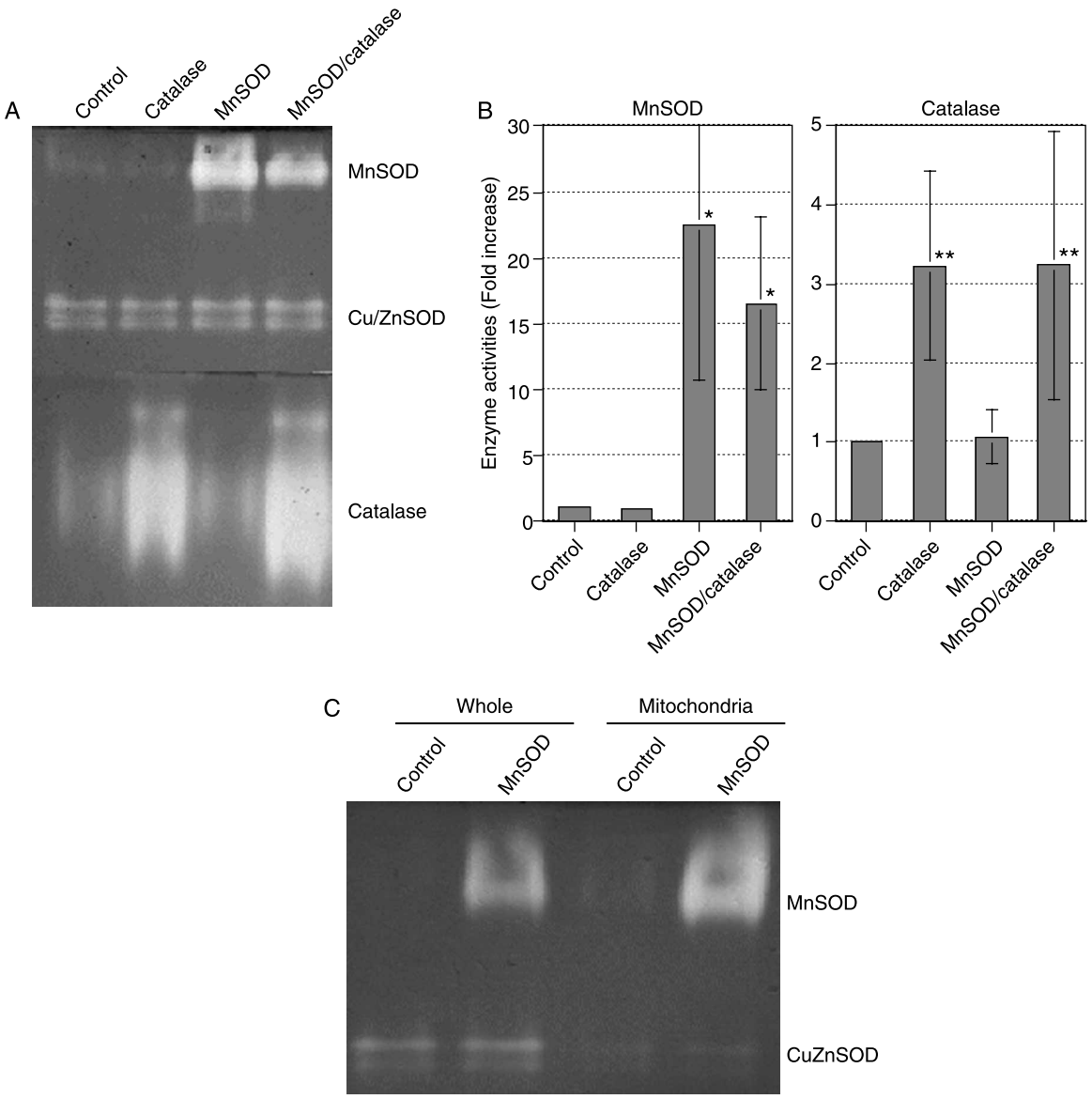

Figure 1. Activities of MnSOD and catalase in SK-HEP-1 cells overexpressing MnSOD and/or catalase. SK-HEP-1 cells were transfected with either human MnSOD, catalase, or MnSOD/catalase cDNA as described in the Materials and Methods. Each tranfectant was sonicated in ice-cold potassium phosphate buffer, 40-μg samples of whole protein were electrophoresed in non-denaturing 12 or 7.5% polyacrylamide gel, and staining was performed with NBT for MnSOD and DAB for catalase. (A) The upper gel was stained for SOD activities and the lower gel for catalase activities. Control, cells transfected with expression vectors; Catalase, cells overexpressing catalase; MnSOD, cells overexpressing MnSOD; MnSOD/catalase, cells overexpressing both MnSOD and catalase. Results are typical of at least three independent experiments. (B) The relative densities of all bands were determined and quantified. Results are means ± SD for three independent experiments. (C) Mitochondrial fractions were isolated from each transfectant. One hundred and twenty micro-grams of sample proteins were electrophoresed and the gel was stained for SOD. $*p < 0.01$ (compared to Control).

with or without full-length human catalase cDNA. Thus, we obtained stable transfectants with either MnSOD, catalase, or MnSOD/catalase following selection by zeocin. We studied the activities of these enzymes in these cells by the native gel assay described in the Materials and Methods. Figure 1 shows typical clones of each of the transfectants. We picked up one clone each showing the most abundant activities of each enzyme. As reported previously, eukaryotes have two types of SOD in cells; the bands of high molecular mass are MnSOD and the very faint bands at low molecular mass correspond to copper-zinc SOD (Cu/ZnSOD) [21]. Cells over-expressing MnSOD or MnSOD/catalase had about 15–20-fold higher activities of MnSOD as compared to control cells. However, there were no differences in activities of Cu/ZnSOD among these cell lines. A study of catalase activity showed that cells introduced with a catalase cDNA had 3-fold higher activity than control. Higher activities of these enzymes remained

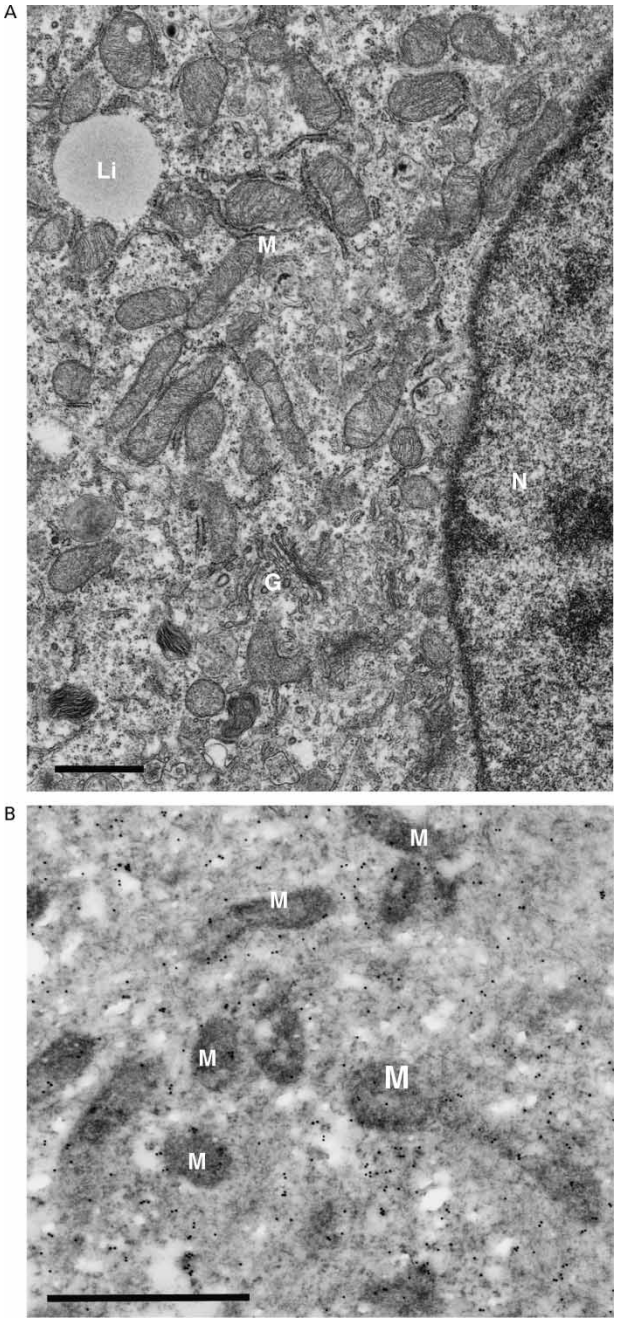

Figure 2. Intracellular localization of catalase. (A) Transmission electron micrograph of SK-HEP-1 cells. Cells were fixed and double stained with uranyl acetate and lead citrate, and then examined by transmission electron microscopy. N, nucleus; M, mitochondria; Li, lipid droplet; G, Golgi apparatus. Bar = 1 μm. (B) Immunoelectron microscopic image of catalase-transfectants. Cells were fixed and reacted with the anti-catalase antibody. Gold spheres (10 nm diameter) indicate catalase molecules. M, mitochondria. Bar = 1 μm.

unaltered during 3-month serial culture (data not shown).

We determined intracellular localization of the stably tranfected MnSOD and catalase proteins in these cells. A mitochondrial fraction was isolated and activities of MnSOD of the mitochondrial fraction were compared in the control cells and MnSOD-transfectants (Figure 1(C)). The MnSOD activity was almost 15–20-fold higher in the mitochondrial fraction of the MnSOD trasfectants than in that of the control cells (Figure 1(C)), suggesting that the overexpressed MnSOD was localized to mitochondria in these cells. Using transmission and immunoelectron microscopy, we also studied intracellular localization of overexpressed catalase in these transfectants (Figure 2). Studies of transmission microscopy found that SK-HEP-1 cells had large numbers of mitochondria, endoplasmic reticulum and lysosomes, but few peroxisomes were observed in these cells (Figure 2(A)). The catalase protein is known to be located within peroxisomes in mammalian cells. However, immunoelectron microscopy experiments showed that catalase was hardly detected in control cells (not shown), whereas a band was detected on a native gel. These were consistent with results of the low catalase activity in control cells. On the other hand, the catalase protein was detected as gold particles conjugated with an antibody in endoplasmic reticulum or cytosol but not in mitochondria in catalase-transfectants (Figure 2(B)). Thus, the introduced catalase protein was not localized to peroxisomes since SK-HEP-1 cells had few peroxisomes.

Production of intracellular H_2O_2 in stable transfectants

Next, we determined whether higher activities of MnSOD and/or catalase affected the levels of intracellular H_2O_2 (Figure 3). The production of H_2O_2 was assessed using a fluorescence probe, CM-H_2DCFDA [22]. FACS analysis revealed mean fluorescent intensities of 205 ± 33, 220 ± 111, 584 ± 190 and 209 ± 44 for control, catalase-, MnSOD-, and MnSOD/catalase-transfectants, respectively. Thus, the MnSOD-transfectants generated significantly higher levels of H_2O_2 than the other cell lines. However, there were no differences among the intensities of the control, catalase-, and MnSOD/-catalase-transfectants.

Role of anti-oxidant enzymes in damage of mtDNA by UV-irradiation

Damage to mtDNA was indicated by the detection of various base modifications. Particularly, 8-oxodGuo is a good marker of mtDNA damage that can lead to point mutations because of mispairing. Detecting 8-oxodGuo, we studied the magnitude of oxidative damage to mtDNA in these cells by UV-irradiation. First, we obtained the mitochondrial fraction from SK-HEP-1 cells by sucrose gradient centrifugation, and then mtDNA was extracted. In order to check the contamination of nuclear DNA in the mtDNA fraction, the G3PDH gene was amplified using PCR (Figure 4). No bands corresponding to G3PDH gene

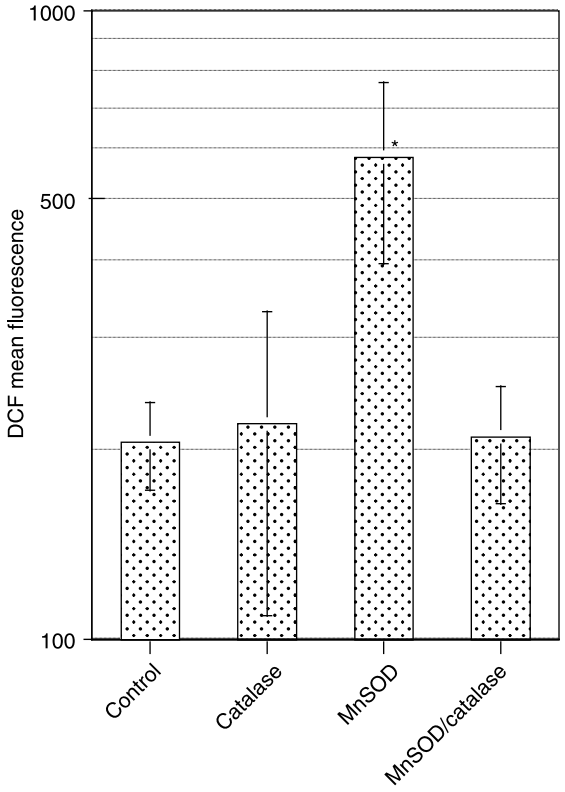

Figure 3. Production of H_2O_2 at steady state in transfectants. Cells were stained with 2 mM of CM-H_2DCFDA, a peroxide-sensitive fluorescent probe, for 15 min at 37°C, and fluorescent intensities were measured by flow cytometry. Results are shown as mean fluorescent intensities ± SD of four independent experiments. $\star p < 0.01$ (compared to Control).

were detected in the mtDNA fraction, whereas clear bands were amplified in the total DNA fraction. Thus, the mtDNA preparation was free of any detectable nuclear DNA by PCR analysis.

UV rays can be classified into the non-solar UVC (100–280 nm), the solar UVB (280–320 nm), and the UVA (320–380 nm) based on the wavelengths. Studies have shown that UVC is well established as a ROS generator in experiments of cells although UVA has a stronger capacity to generate ROS more than UVC [23]. Moreover, short wavelength of UV is strongly absorved by nucleic acids [24]. Cells were irradiated by UVC (254 nm) to generate ROS in cells to investigate accumulations of damages in mtDNA in the present report. To analyze 8-oxodGuo from mtDNA, 10^8 cells were irradiated by UV rays and mtDNA was extracted as described in the Materials and Methods. We used a lethal dose of irradiation with 1 kJ/m^2 to detect damages of mtDNA more clearly. MtDNA was digested by nuclease P1 followed by treatment with bacterial alkaline phosphatase, and then loaded to HPLC-electron chemical detection (HPLC-ECD) system. The contents of 8-oxodGuo and 2dG were evaluated as the area under each peak. We compared the 8-oxodGuo/2dG ratios in the

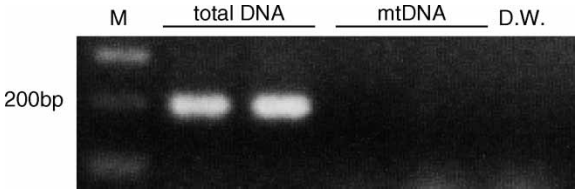

Figure 4. Purity of isolated mtDNA. The purity of isolated mtDNA was determined by PCR amplification using a primer pair designed for amplifying nuclear DNA encoding G3PDH gene. The 196-bp PCR products were tested by 2% agarose gel electrophoresis and stained with ethidium bromide. Total DNA fractions from SK-HEP-1 (lanes 1 and 2), purified mtDNA fractions (lanes 3 and 4) and D.W. (lane 5) were used as PCR templates, and PCR amplification was performed for 30 cycles. M, marker.

mtDNA preparations before and after UV irradiation in each cell line. There were no significant differences in 8-oxodGuo/2dG among control, catalase-, MnSOD-, and catalase/MnSOD-transfectants before

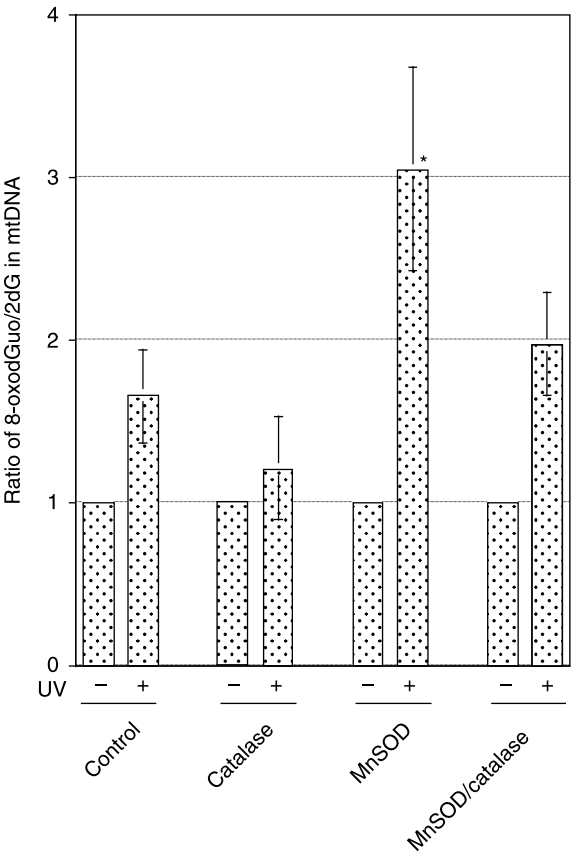

Figure 5. Analysis of mtDNA hydrolysate by HPLC-ECD. Purified mtDNA from cells with or without UV-irradiation were digested with nuclease P1, followed by alkaline phosphatase treatment, and then analysis by HPLC-ECD system. The area under each peak was measured and the amount of 8-oxodGuo was normalized to the amount of 2dG, as determined by HPLC-ECD. The ratio of 8-oxodGuo/2dG of each cell line was summarized and the ratio in untreated cells was taken as baseline. Results are presented as mean ± standard error of 8 independent experiments. The ratios of 8-oxodGuo/10^5 dG in untreated cells were 0.8–2.4. $\star p < 0.001$ (compared to Control).

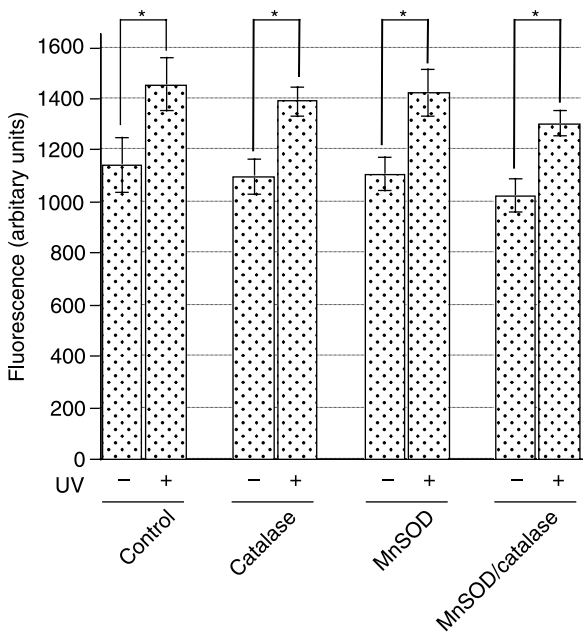

Figure 6. Intracellular levels of chelatable iron. Cells were irradiated with UVC at a dose of 1 kJ/cm^2 and were loaded with 0.05 μM calcein-AM. Then the calcein fluorescence of cells was measured using a spectro-fluorometer with excitation at 488 nm and emission at 517 nm. Results are represented as relative fluorescence. Each value represents mean ± standard error of three independent experiments. $\star p < 0.01$.

UV-irradiation. When the control cells were exposed to UV-irradiation, the 8-oxodGuo/2dG ratio was increased by 1.7 ± 0.3-fold ($p < 0.05$, Figure 5). Introduction of catalase cDNA did not affect the accumulation of 8-oxodGuo by UV-irradiation. In contrast, the overexpression of MnSOD enhanced the accumulation of 8-oxodGuo by UV-irradiation as the 8-oxodGuo/2dG ratio was increased by 3.1 ± 0.6-fold in MnSOD-transfectants ($p < 0.001$). On the other hand, co-transfection with catalase significantly inhibited the increase in the ratio by UV-irradiation as compared to that of MnSOD-transfectants ($p < 0.02$); the increase in the ratio of MnSOD/catalase-transfectants was 2.0 ± 0.3-fold with UV-irradiation.

Table I. Effects of antioxidant enzymes on clonal cell growth after UV-irradiation.

	10 J/m^2 (%)	20 J/m^2 (%)	40 J/m^2 (%)
Control	26 ± 11***,⋆	2 ± 2***,**	0***
MnSOD	36 ± 10***	1 ± 1***	0
Catalase	20 ± 6***	2 ± 2***	0
MnSOD/catalase	60 ± 8⋆	19 ± 6**	2 ± 2***

⋆$p = 0.006$, **$p = 0.004$, ***not significant. Five hundred cells for control cells and catalase-tranfectants, 1000 cells for MnSOD-transfectants, and 200 cells for MnSOD/catalase-transfectants were seeded on 60-mm dishes and incubated for one day. Then, cells were irradiated at indicated doses of UV and cultured for 7 days. The colonies were counted after Giemsa staining. Results are presented as percentages of colony formation capacity of untreated cells. Plating efficiency of untreated cells was 28 ± 1% in control, 18 ± 2% in MnSOD-, 31 ± 4% in catalase-, and 73 ± 6% in MnSOD/catalase-transfectants.

Intracellular iron release after UV-irradiation

UV-irradiation has been reported to induce iron release [25]. 8-oxodGuo can be generated chemically by hydroxyl radical attack at the C-8 position of guanine [26,27] and the production of hydroxyl radical is mediated by metal ions such as iron ion. In order to determine whether the intracellular iron release is involved in the formation of 8-oxodGuo in mtDNA by UV-irradiation, we measured intracellular levels of released iron in these cell lines after UVC-irradiation. Using calcein-AM, we have compared the released levels of intracellular iron in four cell lines after UV- irradiation (Figure 6) [28]. At a steady state, there were no significant differences in levels of intracellular chelatable iron among the control, catalase-, MnSOD-, and MnSOD/catalase-transfectants. UVC-irradiation increased the release of intracellular iron significantly in each cell line. However, there was no significant difference in the increased levels of iron in these UVC-irradiated cell lines.

Effects of mtDNA damage on cell growth by UV-irradiation

We have shown that the accumulation of H_2O_2 leads to mtDNA damage in UV-irradiation. We sought to determine if the accumulation of H_2O_2 by UV-irradiation affects cell growth in these cells. We determined the effects of UV-irradiation on clonogenic cell growth in these transfectants. First, we compared the clonogenic cell growth in these transfectants at a steady state. Two hundred to a thousand of each transfectant were seeded in a 60-mm culture dish and cultured for 10 days. Control, catalase-, MnSOD-, and MnSOD/catalase-transfectants had colony forming capacities of 28 ± 1, 31 ± 4, 18 ± 2 and 73 ± 6%, respectively. These results suggest that the overexpression of MnSOD inhibits cell growth ($p < 0.005$) and the overexpression of both catalase and MnSOD enhances cell growth ($p < 0.0001$). However, the overexpression of catalase had no effect on clonal cell growth. Studies of cell growth rate by spectrophotometric analysis using WST staining showed quite similar results (data not shown).

In order to study the effects of UV-irradiation on the growth of these transfectants, cells were plated and then irradiated at a dose of 10, 20 and 40 J/m^2. UV-irradiation inhibited the colony forming capacity of the control cells in a dose-dependent manner; 10, 20 and 40 J/m^2 of UV reduced the capacity to 26 ± 11, 2 ± 2 and 0% of untreated cells, respectively (Table I).

Similar results were observed in MnSOD- and catalase-transfectants upon UV-irradiation; no differences were observed in capacity among control, MnSOD- and catalase-transfectants at any of the irradiation levels. In contrast, the overexpression of MnSOD/catalase significantly rescued the inhibition of colony forming capacity by UV-irradiation. Upon UV-irradiation with 10 and 20 J/m^2, MnSOD/catalase-transfectants had colony forming abilities of 60 ± 8 and 19 ± 6%, respectively.

Discussion

ROS are generated not only as a byproduct of normal respiration but also by external insults such as ionizing and UV-irradiation. ROS are known to cause damage to nuclear and mtDNA, resulting in genetic mutations. On the other hand, recent studies have revealed important roles of ROS in redox signaling [29]. Mitochondrial structures are continuously exposed to high concentrations of ROS, and studies have found mutations of mtDNA in various organs such as skeletal muscle and the central nervous system [30,31]. We examined the role of H_2O_2 in the damage to mtDNA by UV-irradiation in SK-HEP-1 hepatoma cells. Measuring the levels of 8-oxodGuo by HPLC, we showed that the introduction of MnSOD gene enhanced the damage of mtDNA in UV-irradiated cells, and the co-introduction of catalase gene reduced the damage. Moreover, the accumulation of H_2O_2 by MnSOD inhibited cell growth. However, co-introduction of catalase cDNA into MnSOD-transfectants led to growth stimulation. In the present study, we showed for the first time that mtDNA damage is caused primarily through H_2O_2 rather than $O_2^{\cdot-}$ in UV-irradiation.

The primary cellular enzymatic defense systems against H_2O_2 are catalase, peroxiredoxins and the glutathione redox cycle; these enzymes catalyze H_2O_2 to H_2O and O_2. Catalase is one of the most efficient enzymes for the detoxication of H_2O_2, but it is present only or primarily in peroxisomes, although it has been found in mitochondria of cardiac cells [32]. In mitochondria, known enzymatic defenses against H_2O_2 are the glutathione redox cycle system and peroxiredoxins. Due to membrane permeability, however, H_2O_2 can pass through mitochondrial membranes freely to the cytoplasm, and manipulation of H_2O_2 production in cytosol results in changes to the amount of extracellular and mitochondrial H_2O_2, leading to a variety of biological modifications. Thus, H_2O_2 in mitochondria has unlimited access to the peroxisomal enzyme. In the present study, we assessed the production of ROS using the fluorescent probe CM-H_2DCFDA. This method is not specific for H_2O_2 and reacts with ROS other than H_2O_2. Co-overexpression of catalase reduced the ROS production in the cells overexpressing MnSOD. Since SOD catalyzes the dismutation of $O_2^{\cdot-}$ to H_2O_2 and substrate of catalase is H_2O_2, our results suggest that the generation of ROS at a steady state is increased in MnSOD transfectants than in control cells and that the ROS responsible for MnSOD overexpression is likely H_2O_2. We showed that the accumulation of H_2O_2 by the overexpression of MnSOD increased mtDNA damage, and dismutation of H_2O_2 by the co-expression of catalase ameliorated the damage to mtDNA by UV. We also studied levels of peroxiredoxin I, which is located in the cytosol, and peroxiredoxin III, which is located in the mitochondria. There was no difference in levels of peroxiredoxins I or III among these four cell lines (data not shown). There are many studies of ROS, such as H_2O_2 being implicated in carcinogenesis, aging and various diseases especially for muscle and nerve tissues [33,34]. However, the mechanisms for H_2O_2 accumulation leading to these events are not clear, since H_2O_2 acts only transiently and locally inside the cell, and its concentration in cells is extremely low. Furthermore, the components of ROS responsible for the damage to mtDNA have yet to be identified. In the present study, we showed for the first time that H_2O_2 rather than $O_2^{\cdot-}$ plays an important role in mtDNA injury upon UV-irradiation. The mitochondrial respiratory chain generates primarily $O_2^{\cdot-}$ and consequently H_2O_2, either as a product of SODs or by spontaneous disproportionation. In the presence of reduced transition metals such as ferrous or cuprous ions, H_2O_2 can be converted into the highly reactive hydroxy radical ($^{\cdot}OH$) [35,36]. On the other hand, H_2O_2 is thought to be relatively less reactive for DNA [36]. H_2O_2 is relatively stable compared to other ROS molecules; the half- life of H_2O_2 is 1 milli-second and that of $O_2^{\cdot-}$ is 1 micro-second [37]. Thus, the clearance rate of each component of ROS may induce the imbalance of ROS, leading to the disturbance of redox homeostasis in mitochondria.

Damage by oxidative stress to mitochondrial components includes lipid peroxidation, protein oxidation and damaged mtDNA. Especially the oxidative attack from ROS of mitochondrial origin is among the primary possible causes of mtDNA damage. 8-oxodGuo is a highly mutagenic lesion, since it can mispair with A, leading to a G:C - > A:T transversion [1]. Studies have found that relatively higher steady-state levels of 8-oxodGuo are observed in short-lived animals such as rodents and in old individuals, suggesting a higher risk of mutations in their mtDNA [38]. Moreover, previous reports revealed an accumulation of deleted mutations in mtDNA after UV-irradiation [15,39,40]. In the present study, we determined the level of 8-oxodGuo as a marker of damage to mtDNA using the HPLC-ECD system. A common problem when measuring oxidative DNA damage is the introduction of artificial modifications during DNA isolation.

A source of the most artificial oxidative damage to DNA molecule is phenol treatment. We used silica-gel membrane without organic extraction for mtDNA to minimize artificial oxidative damage. Moreover, UV-irradiation is known to induce intracellular iron release, causing iron-mediated damage [41,42]. We assessed the levels of intracellular chelatable iron in these transfectants. However, overexpression of catalase, MnSOD, or catalase/MnSOD did not affect the increased levels of intracellular chelatable iron by UV-irradiation. These results indicate that the release of intracellular iron is not related to the accumulation of 8-oxodGuo from mtDNA of MnSOD-transfectants by UV-irradiation. Contamination with nuclear DNA is also a common problem for analysis of mtDNA. Since the content of 8-oxodGuo is also considered a marker of oxidative damage to nuclear DNA [43], we purified mtDNA after treatment of the mitochondrial fraction with DNase I to digest nuclear DNA contaminated in the fraction [19]. However, nuclear DNA encoding G3PDH was not detected in DNA extracted from the mitochondrial fraction, whereas a 196 bp fragment of DNA was amplified in the control. Thus, the mtDNA preparation was free of any detectable nuclear DNA.

It has been proposed that the accumulation of somatic mutations of mtDNA, induced by exposure to ROS, may lead to errors in mtDNA-encoded polypeptides; such errors are stochastic and randomly transmitted during mitochondrial division and cell division. The mitochondrial theory of aging postulates that random alterations of mtDNA in somatic cells are responsible for the energetic decline accompanying senescence [44]. Moreover, there is accumulating evidence that mtDNA is a target of age-associated ROS [45]. Some mutations of mtDNA lead to impaired respiratory function. Furthermore, it has been suggested that impairment of the respiratory chain increases the production of ROS including H_2O_2 in mitochondria, thus establishing a vicious circle of mtDNA damage and oxidative stress [46]. In the present study, the overexpression of MnSOD inhibited the growth of SK-HEP-1 cells, with concomitantly increased levels of H_2O_2. These results are consistent with our previous report concerning other types of cells [17], and support the hypothesis that ROS, especially H_2O_2, could control cell proliferation and cell division [47]. It has also been shown that cells exhibiting an increase in the ratio of Cu/ZnSOD to catalase had typical features of cellular senescence, as indicated by a slower growth rate [48]. In our study, however, cells overexpressing both MnSOD and catalase had stronger proliferative activities than control cells and other cell lines, whereas there were no significant differences in H_2O_2 levels among control cells, MnSOD-transfectants and catalase-transfectants. The mechanisms for the activation of cell proliferation in these cells are not clear. In our study, on the other hand, the overexpression of MnSOD did not affect the growth inhibition by UV-irradiation, while MnSOD enhanced the damage to mtDNA by UV and the co-overexpression with catalase reduced it. The magnitude of damage to mtDNA by H_2O_2 appears to be not directly related to the inhibition of growth in these cells. While the accumulation of H_2O_2 causes the mtDNA damage in UV-irradiation, the fate of cell growth or death may be regulated through more complicated mechanisms dependent on balance in each component of ROS in the entire cell.

In the present study, we have shown the role of catalase in the protection against ROS damaging mtDNA under UV exposure, while the overexpression of MnSOD enhanced oxidative damage to mtDNA in UV exposure. Cells overexpressing Cu/ZnSOD have been shown to have a higher level of lipid peroxidation than control cells [49]. Furthermore, MnSOD enhanced oxidative damage to DNA *in vitro* [50]. However, it has also been reported that the amount of mtDNA mutations was increased in mice lacking cytosolic SOD, suggesting that SOD acts as a protector against ROS in mitochondria [51]. Moreover, the overexpression of MnSOD increases the cellular resistance to oxidative damage [18]. The reasons for these discrepancies among studies are unclear. Unlike H_2O_2, $O_2^{\cdot-}$ in cytosol cannot freely permeate the mitochondrial membrane. Therefore, a fine balance between enzymes scavenging ROS is important for the cellular resistance to oxidative stress [52]. Modification of the redox state in mitochondria may be an important regulatory mechanism for DNA injury by UV-irradiation.

References

[1] Grollman AP, Moriya M. Mutagenesis by 8-oxoguanine: An enemy within. Trends Genet 1993;9:246–249.
[2] Boveris A, Oshino N, Chance B. The cellular production of hydrogen peroxide. Biochem J 1972;128:617–630.
[3] Papa S. Mitochondrial oxidative phosphorylation changes in the life span. Molecular aspects and physiopathological implications. Biochim Biophys Acta 1996;1276:87–105.
[4] Stadtman ER. Protein oxidation and aging. Science 1992;257:1220–1224.
[5] Hirose K, Longo DL, Oppenheim JJ, Matsushima K. Overexpression of mitochondrial manganese superoxide dismutase promotes the survival of tumor cells exposed to interleukin-1, tumor necrosis factor, selected anticancer drugs, and ionizing radiation. FASEB J 1993;7:361–368.
[6] Wispe JR, Warner BB, Clark JC, Dey CR, Neuman J, Glasser SW, Crapo JD, Chang LY, Whitsett JA. Human Mn-superoxide dismutase in pulmonary epithelial cells of transgenic mice confers protection from oxygen injury. J Biol Chem 1992;267:23937–23941.
[7] Clayton DA. Transcription of the mammalian mitochondrial genome. Annu Rev Biochem 1984;53:573–594.
[8] Larsson NG, Clayton DA. Molecular genetic aspects of human mitochondrial disorders. Annu Rev Genet 1995;29:151–178.
[9] Wallace DC. Mitochondrial diseases in man and mouse. Science 1999;283:1482–1488.

[10] Raha S, Robinson BH. Mitochondria, oxygen free radicals, disease and ageing. Trends Biochem Sci 2000;25:502–508.
[11] Richter C, Park JW, Ames BN. Normal oxidative damage to mitochondrial and nuclear DNA is extensive. Proc Natl Acad Sci USA 1988;85:6465–6467.
[12] Beckman KB, Ames BN. Detection and quantification of oxidative adducts of mitochondrial DNA. Methods Enzymol 1996;264:442–453.
[13] Farber JL. Mechanisms of cell injury by activated oxygen species. Environ Health Perspect 1994;102:17–24.
[14] Peus D, Vasa RA, Beyerle A, Meves A, Krautmacher C, Pittelkow MR. UVB activates ERK1/2 and p38 signaling pathways via reactive oxygen species in cultured keratinocytes. J Invest Dermatol 1999;112:751–756.
[15] Berneburg M, Grether-Beck S, Kurten V, Ruzicka T, Briviba K, Sies H, Krutmann J. Singlet oxygen mediates the UVA-induced generation of the photoaging-associated mitochondrial common deletion. J Biol Chem 1999;274:15345–15349.
[16] Kawasaki K, Suzuki T, Ueda M, Ichihashi M, Reguer G, Yamasaki H. CC to TT mutation in the mitochondrial DNA of normal skin: Relationship to ultraviolet light exposure. Mutat Res 2000;468:35–43.
[17] Takada Y, Hachiya M, Park SH, Osawa Y, Ozawa T, Akashi M. Role of reactive oxygen species in cells overexpressing manganese superoxide dismutase: Mechanism for induction of radioresistance. Mol Cancer Res 2002;1:137–146.
[18] Attardi G, Ching E. Biogenesis of mitochondrial proteins in HeLa cells. Methods Enzymol 1979;56:66–79.
[19] Ausenda C, Chomyn A. Purification of mitochondrial DNA from human cell cultures and placenta. Methods Enzymol 1996;264:122–128.
[20] Mancini M, Anderson BO, Caldwell E, Sedghinasab M, Paty PB, Hockenbery DM. Mitochondrial proliferation and paradoxical membrane depolarization during terminal differentiation and apoptosis in a human colon carcinoma cell line. J Cell Biol 1997;138:449–469.
[21] Suzuki YJ, Forman HJ, Sevanian A. Oxidants as stimulators of signal transduction. Free Radic Biol Med 1997;22:269–285.
[22] Myhre O, Andersen JM, Aarnes H, Fonnum F. Evaluation of the probes 2′,7′-dichlorofluorescin diacetate, luminol, and lucigenin as indicators of reactive species formation. Biochem Pharmacol 2003;65:1575–1582.
[23] Matsuda N, Horikawa M, Wang LH, Yoshida M, Okaichi K, Okumura Y, Watanabe M. Differential activation of ERK 1/2 and JNK in normal human fibroblast-like cells in response to UVC radiation under different oxygen tensions. Photochem Photobiol 2000;72:334–339.
[24] Tyrrell RM. Activation of mammalian gene expression by the UV component of sunlight—from models to reality. Bioessays 1996;18:139–148.
[25] Pourzand C, Watkin RD, Brown JE, Tyrrell RM. Ultraviolet A radiation induces immediate release of iron in human primary skin fibroblasts: The role of ferritin. Proc Natl Acad Sci USA 1999;96:6751–6756.
[26] Schneider JE, Price S, Maidt L, Gutteridge JM, Floyd RA. Methylene blue plus light mediates 8-hydroxy 2′-deoxyguanosine formation in DNA preferentially over strand breakage. Nucleic Acids Res 1990;18:631–635.
[27] Greenberg MM. *In vitro* and *in vivo* effects of oxidative damage to deoxyguanosine. Biochem Soc Trans 2004;32:46–50.
[28] Gau RJ, Yang HL, Suen JL, Lu FJ. Induction of oxidative stress by humic acid through increasing intracellular iron: A possible mechanism leading to atherothrombotic vascular disorder in blackfoot disease. Biochem Biophys Res Commun 2001;283:743–749.
[29] Droge W. Free radicals in the physiological control of cell function. Physiol Rev 2002;82:47–95.
[30] Hayakawa M, Torii K, Sugiyama S, Tanaka M, Ozawa T. Age-associated accumulation of 8-hydroxydeoxyguanosine in mitochondrial DNA of human diaphragm. Biochem Biophys Res Commun 1991;179:1023–1029.
[31] Mecocci P, MacGarvey U, Kaufman AE, Koontz D, Shoffner JM, Wallace DC, Beal MF. Oxidative damage to mitochondrial DNA shows marked age-dependent increases in human brain. Ann Neurol 1993;34:609–616.
[32] Radi R, Turrens JF, Chang LY, Bush KM, Crapo JD, Freeman BA. Detection of catalase in rat heart mitochondria. J Biol Chem 1991;266:22028–22034.
[33] Dreher D, Junod AF. Role of oxygen free radicals in cancer development. Eur J Cancer 1996;32A:30–38.
[34] Knight JA. Advances in the analysis of cerebrospinal fluid. Ann Clin Lab Sci 1997;27:93–104.
[35] Cadenas E, Davies KJ. Mitochondrial free radical generation, oxidative stress, and aging. Free Radic Biol Med 2000;29: 222–230.
[36] Beckman KB, Ames BN. The free radical theory of aging matures. Physiol Rev 1998;78:547–581.
[37] Reth M. Hydrogen peroxide as second messenger in lymphocyte activation. Nat Immunol 2002;3:1129–1134.
[38] Michikawa Y, Mazzucchelli F, Bresolin N, Scarlato G, Attardi G. Aging-dependent large accumulation of point mutations in the human mtDNA control region for replication. Science 1999;286:774–779.
[39] Ray AJ, Turner R, Nikaido O, Rees JL, Birch-Machin MA. The spectrum of mitochondrial DNA deletions is a ubiquitous marker of ultraviolet radiation exposure in human skin. J Invest Dermatol 2000;115:674–679.
[40] Pang CY, Lee HC, Yang JH, Wei YH. Human skin mitochondrial DNA deletions associated with light exposure. Arch Biochem Biophys 1994;312:534–538.
[41] Tyrrell R. Redox regulation and oxidant activation of heme oxygenase-1. Free Radic Res 1999;31:335–340.
[42] Reelfs O, Tyrrell RM, Pourzand C. Ultraviolet a radiation-induced immediate iron release is a key modulator of the activation of NF-kappaB in human skin fibroblasts. J Invest Dermatol 2004;122:1440–1447.
[43] Lenaz G. Role of mitochondria in oxidative stress and ageing. Biochim Biophys Acta 1998;1366:53–67.
[44] Linnane AW, Marzuki S, Ozawa T, Tanaka M. Mitochondrial DNA mutations as an important contributor to ageing and degenerative diseases. Lancet 1989;1:642–645.
[45] Mandavilli BS, Santos JH, Van Houten B. Mitochondrial DNA repair and aging. Mutat Res 2002;509:127–151.
[46] Ozawa T. Genetic and functional changes in mitochondria associated with aging. Physiol Rev 1997;77:425–464.
[47] Burdon RH. Control of cell proliferation by reactive oxygen species. Biochem Soc Trans 1996;24:1028–1032.
[48] de Haan JB, Cristiano F, Iannello R, Bladier C, Kelner MJ, Kola I. Elevation in the ratio of Cu/Zn-superoxide dismutase to glutathione peroxidase activity induces features of cellular senescence and this effect is mediated by hydrogen peroxide. Hum Mol Genet 1996;5:283–292.
[49] Elroy-Stein O, Bernstein Y, Groner Y. Overproduction of human Cu/Zn-superoxide dismutase in transfected cells: Extenuation of paraquat-mediated cytotoxicity and enhancement of lipid peroxidation. Embo J 1986;5:615–622.
[50] Midorikawa K, Kawanishi S. Superoxide dismutases enhance H_2O_2-induced DNA damage and alter its site specificity. FEBS Lett 2001;495:187–190.
[51] Zhang X, Han D, Ding D, Dai P, Yang W, Jiang S, Salvi RJ. Deletions are easy detectable in cochlear mitochondrial DNA of Cu/Zn superoxide dismutase gene knockout mice. Chin Med J (Engl) 2002;115:258–263.
[52] Fukagawa NK. Aging: Is oxidative stress a marker or is it causal? Proc Soc Exp Biol Med 1999;222:293–298.